



**Airborne
determination of the
temporo-spatial
distribution**

M. D Shaw et al.

Airborne determination of the temporo-spatial distribution of benzene, toluene, nitrogen oxides and ozone in the boundary layer across Greater London, UK

M. D. Shaw¹, J. D. Lee², B. Davison¹, A. Vaughan², R. M. Purvis², A. C. Lewis², and C. N. Hewitt¹

¹Lancaster Environment Centre, Lancaster University, Lancaster, UK

²National Centre for Atmospheric Science, University of York, York, UK

Received: 24 September 2014 – Accepted: 15 October 2014 – Published: 30 October 2014

Correspondence to: C. N. Hewitt (n.hewitt@lancaster.ac.uk)

Published by Copernicus Publications on behalf of the European Geosciences Union.

Title Page

Abstract

Introduction

Conclusions

References

Tables

Figures



Back

Close

Full Screen / Esc

Printer-friendly Version

Interactive Discussion



Abstract

Highly spatially resolved mixing ratios of benzene and toluene, nitrogen oxides (NO_x) and ozone (O_3) were measured in the atmospheric boundary layer above Greater London during the period 24 June to 9 July 2013 using a Dornier 228 aircraft. Toluene and benzene were determined in-situ using a proton transfer reaction mass spectrometer (PTR-MS), NO_x by dual channel NO_x chemiluminescence and O_3 mixing ratios by UV absorption.

Average mixing ratios observed over inner London at 360 ± 10 m.a.g.l. were 0.20 ± 0.05 , 0.28 ± 0.07 , 13.2 ± 8.6 , 21.0 ± 7.3 and 34.3 ± 15.2 ppbv for benzene, toluene, NO , NO_2 and NO_x respectively. Linear regression analysis between NO_2 , benzene and toluene mixing ratios yielded a trimodal distribution indicating that these compounds predominantly share the same or co-located sources within the city and that a significant fraction of NO_x is directly emitted as NO_2 .

Average mixing ratios measured at 360 ± 10 m.a.g.l. over outer London were always lower than over inner London. Where traffic densities were highest, the toluene/benzene (T/B) concentration ratios were highest (average of 1.8 ± 0.3 ppbv ppbv⁻¹) indicative of strong local sources. Daytime maxima in NO_x , benzene and toluene mixing ratios were observed in the morning (~ 40 ppbv NO_x , ~ 350 pptv toluene and ~ 200 pptv benzene) and for ozone in the mid-afternoon (~ 40 ppbv O_3) all at 360 ± 10 m.a.g.l.

1 Introduction

Ground level ozone (O_3) is a secondary pollutant, produced from photochemical reactions involving volatile organic compounds (VOCs) and nitrogen oxides ($\text{NO}_x = \text{NO} + \text{NO}_2$). Ozone has significant detrimental effects on human health and vegetation while NO_2 and some VOCs also have, themselves, direct effects on health. Whilst the basic atmospheric chemistry leading to O_3 formation is generally well un-

ACPD

14, 27335–27371, 2014

Airborne determination of the temporo-spatial distribution

M. D Shaw et al.

Title Page

Abstract

Introduction

Conclusions

References

Tables

Figures

◀

▶

◀

▶

Back

Close

Full Screen / Esc

Printer-friendly Version

Interactive Discussion



derstood, there are substantial uncertainties associated with the magnitude and speciation of emissions of both VOCs and NO_x from urban areas, leading to uncertainties in the detailed understanding of urban photochemistry and air pollution.

In urban areas the dominant anthropogenic sources of VOCs are vehicular exhaust, fuel evaporation and emissions from the commercial and industrial use of solvents (Nelson et al., 1983). Vehicular emissions are the predominant source of VOCs to the atmosphere in urban and suburban areas, accounting for > 50 % of the total (Na et al., 2005; Kansal, 2009; Watson et al., 2001) with a wide range of VOCs emitted directly due to fuel evaporation and from vehicular exhaust as unburnt fuel and as partially oxidized fuel components. The dominant urban sources of NO_x are combustion processes, including vehicles. In the UK as a whole, about 50 % of NO_x is thought to be derived from vehicles, although this percentage is larger in urban areas.

In the UK, spatially disaggregated NO_x and VOC emission rates are estimated by the National Atmospheric Emission Inventory (NAEI), which provides emission estimates for specific pollutants by source sector at 1 km^2 resolution. Uncertainties in these emission estimates propagate through into uncertainties in models of air quality, and leads to uncertainties in the likely effectiveness of control policies on both background and peak VOCs, O_3 and NO_2 mixing ratios in the UK. There are therefore considerable economic and societal pressures to ensure the precision and accuracy of these emissions estimates.

Validation of the NAEI emission estimates is provided, indirectly and in part, by the continuous hourly data of VOC and NO_x mixing ratios measured in the national monitoring networks (the Automatic Hydrocarbon Network (AHN) and the Automatic Urban and Rural Network (AURN), both operated by the Department of Environment, Food and Rural Affairs). Hourly mixing ratios of NO_x species are currently measured at 130 network sites with selected VOCs measured at 4 sites. Within Greater London these sites form part of the London Air Quality Network (LAQN). However, these networks only measure mixing ratios and suffer from the limitations of being made at relatively few sites and so may not be representative of mixing ratios over larger spatial scales.

Airborne determination of the temporo-spatial distribution

M. D Shaw et al.

[Title Page](#)[Abstract](#)[Introduction](#)[Conclusions](#)[References](#)[Tables](#)[Figures](#)[Back](#)[Close](#)[Full Screen / Esc](#)[Printer-friendly Version](#)[Interactive Discussion](#)

Airborne determination of the temporo-spatial distribution

M. D Shaw et al.

Title Page

Abstract

Introduction

Conclusions

References

Tables

Figures



Back

Close

Full Screen / Esc

Printer-friendly Version

Interactive Discussion



The development of fast-response analytical instruments for NO_x and VOCs means that the mixing ratios of these analytes can now be measured at high spatial resolution from low-flying aircraft. The advantages of in-situ aircraft measurements is that they provide information on the horizontal and vertical distributions of air pollutants over a large spatial area allowing continuous gradients of mixing ratios to be observed across cities and their surrounding rural areas.

In this study, we investigate the mixing ratios of O₃, benzene, toluene, NO, NO₂ and NO_x across the Greater London region during several flights using the Natural Environment Research Council (NERC) Atmospheric Research and Survey Facility Dornier 228 aircraft between 24 June and 9 July 2013. The aim of this work was to (i) quantitatively determine the vertical, horizontal spatial and temporal distribution of VOCs, NO_x and ozone mixing ratios across London from an airborne platform, with a view to identify dominant emission sources in the region and (ii) wherever possible, compare these fast response airborne measurements with hourly ground-level measurements made by the national monitoring networks.

2 Method

2.1 NERC Dornier 228

The NERC Dornier 228 is a twin-engine turbo-prop powered, none pressurised aircraft operated by the Airborne Research and Survey Facility (ARSF) based at Gloucester airport in central England. The aircraft has a cabin volume of 14 m³ and operated with a crew of 2 pilots and 4 scientists for the duration of the flights. The aircraft has a minimum and maximum airspeed of 65 and 95 m s⁻¹ respectively producing maximum range of 2400 km (5 h at 500 kg). The aircraft has a maximum payload of 5970 kg including fuel, with a maximum operational altitude for science of 4500 m.

2.2 Flight description

Eleven research flights (RF) totalling 45 h in duration were conducted between the hours of 8:30–17:20 UTC (Table 1). Figure 1a shows all flight legs conducted during the project, overlaid on a transport map of SE England. Here we will focus on data obtained in transects across London (~ 27 h of research flights). Figure 1b shows a map of Greater London on which typical repeated south-westerly to north-easterly flight legs of ~ 50 km are plotted. Identical flight legs across Greater London were chosen due to tight air traffic regulations and to allow data analysis in both a temporal and spatial domain. The grey area represents the Greater London boundary, the black area the inner London boundary and the blue area London's congestion charging zone (CCZ) in which road traffic is heavily regulated and subject to financial charging. Airspeed and altitude were fixed during the flights across Greater London with mean values of $73 \pm 3 \text{ m s}^{-1}$ and $360 \pm 10 \text{ m a.g.l.}$ respectively (Table 1).

The predominant wind directions observed during the flights were either north-westerly (RF 1–6), perpendicular to the flight transects, or north-easterly (RF 7–10), parallel to the flight transects (Table 1). Perpendicular wind directions are useful in providing a cross section of pollutant mixing ratios across London. Parallel wind directions allow us to assess the horizontal advection and dispersion of pollutants across the city and their transport to suburban and rural regions. RF 1 focussed on vertically profiling the PBL above London.

Boundary layer (BL) height determinations were made from a combination of airborne observations and ground based measurements. Approximately hourly lower cloud base altitude determinations were made from Heathrow airport using laser cloud based recorder (LCBR) observations. The lowest observed cloud base was interpreted as BL height. Where cloud based observations were not available (during clear skies), temporally interpolated BL height determinations from aircraft observations were used. Briefly, before commencing the city transects, a spiral descent from 2500 to 350 m a.g.l. was performed 70 km south of London (position BL 1, Fig. 1b). Similarly, immediately

Airborne determination of the temporo-spatial distribution

M. D Shaw et al.

Title Page

Abstract

Introduction

Conclusions

References

Tables

Figures



Back

Close

Full Screen / Esc

Printer-friendly Version

Interactive Discussion



after completing the city transects, a spiral ascent from 350 to 2500 m was performed directly north of London (position BL 2, Fig. 1b). These manoeuvres were performed to determine the height of the BL before and after the flights.

2.3 Meteorological and GPS sampling

5 Core equipment on the aircraft consisted of an Aircraft Integrated Meteorological Measurement System (AIMMS-20) turbulence probe (Aventech Research Inc.) mounted in an underwing PMS type pylon. The instrument is capable of precisely defining the aircraft altitude and velocity to within fractions of one metre per second with a temperature and humidity measurement precision of approximately 1%. This information is
10 combined with fully compensated air-data measurements to compute wind speed with an accuracy of 0.5 knot and wind direction accuracy of 5–10° (Beswick et al., 2008). The 3-D position of the aircraft was measured using an IPAS 20 (Leica) inertial position and altitude system at an accuracy of 0.05–0.3 m. All variables were acquired at a data acquisition rate of 20 Hz.

15 2.4 NO_x sampling

NO_x was measured from the aircraft using a fast time resolution (10 Hz), high sensitivity NO_x chemiluminescence system built by Air Quality Design, Inc. The instrument has a dual channel architecture for independent quantification of NO and NO₂. Each channel has a sample flow of 1.5 L min⁻¹ to ensure the required fast response time.
20 A detailed review of similar system was described by (Lee et al., 2009), being a single channel instrument which operate using the same principles at the Cape Verde Atmospheric Observatory. NO₂ was quantified in a second channel by photolytic conversion to NO using blue light LED diodes centred at 395 nm. The 395 nm wavelength has a specific affinity for NO₂ photolytic conversion to NO, giving high analyte selectivity
25 within the channel. Recent work (Pollack et al., 2010) evaluated the relative high NO₂ affinity for conversion of NO₂ to NO using 395 nm blue light LED's. They highlighted the

Airborne determination of the temporo-spatial distribution

M. D Shaw et al.

Title Page

Abstract

Introduction

Conclusions

References

Tables

Figures

◀

▶

◀

▶

Back

Close

Full Screen / Esc

Printer-friendly Version

Interactive Discussion



Airborne determination of the temporo-spatial distribution

M. D Shaw et al.

Title Page

Abstract

Introduction

Conclusions

References

Tables

Figures



Back

Close

Full Screen / Esc

Printer-friendly Version

Interactive Discussion



low probability of other species within the gaseous chemical matrices such as nitrous acid (HONO), being affected by the 395 nm light, so in turn reducing possible non NO₂ species interfering with the measurement. NO_x was then quantified by ozonation of the subsequent total NO present in the reaction vessel after conversion with NO₂ derived from the difference between NO_x and NO mixing ratios.

The instrument was calibrated by adding a small a flow (5 sccm) of a known NO concentration (5 ppmv – Air Liquide) in the ambient sample flow, resulting in around 10 ppbv of NO. The conversion efficiency of the NO₂ converter was measured during each calibration by gas phase titration of the NO to NO₂ by addition of O₃. NO₂ mixing ratio data is corrected for using the measured 90 % photolytic conversion efficiency. In flight calibrations were always carried out above the boundary layer, thus ensuring low and stable background levels of NO_x. Typically calibrations are carried out at the beginning and end of a flight, with sensitivities and conversion efficiency interpolated between the two and applied to all data. Detection limits for the 1 Hz data were ~ 75 pptv for NO and 100 pptv for NO₂ with approximate total errors at 1 ppbv being 10 and 15 % for NO and NO₂ respectively.

2.5 Ozone sampling

Ozone was quantified in-situ, using a Thermo Scientific 49i UV absorption instrument generating data every 4 s. A mercury lamp emitting UV light was used, with absorption at 254 nm being proportional to O₃ concentration. The measurement uncertainty was estimated to be ±0.8 ppbv.

2.6 VOC sampling

Benzene and toluene mixing ratios were determined simultaneously using an Ionicon (Innsbruck, Austria) high sensitivity proton transfer reaction mass spectrometer (PTR-MS) fitted with a stainless steel ringed drift tube (9.6 cm) and three Pfeiffer turbo-molecular pumps. This instrument has been described in detail elsewhere (Karl et al.,

**Airborne
determination of the
temporo-spatial
distribution**

M. D Shaw et al.

Title Page

Abstract

Introduction

Conclusions

References

Tables

Figures



Back

Close

Full Screen / Esc

Printer-friendly Version

Interactive Discussion



2009; de Gouw and Warneke, 2007; Hewitt et al., 2003; Hayward et al., 2002). Therefore only instrument set up, operation and flight modifications are outlined here. The instrument, normally housed in one cabinet, had been re-engineered by the manufacturers into two racks suitable for mounting into the aircraft. To mitigate shock and vibration to the PTR-MS during flight, the instrument racks, mass spectrometer and MD4 diaphragm pump were individually shock mounted using stainless steel spring mountings (vibrachoc). A pressure controller was added (Bronkhorst) which regulates the inlet flow (50–500 STP sccm), such that pressure upstream of the controller is maintained at a constant value. As a result the PTR-MS drift tube pressure is independent of fluctuations in ambient pressure caused by varying flight altitude. Ambient sample air was only exposed to heated (70 °C) Teflon and stainless steel tubing, minimizing memory effects, inlet losses and the build-up of impurities in the inlet system. Considerable efforts were made to prevent VOC contamination of the PTR-MS inlet during operation on the ground and during take-off. On the ground the PTR-MS inlet remained closed (and all sample tubing capped). Approximately 3 h before each flight the instrument voltages were switched on to allow for primary ion count stabilisation and instrument calibration. During this time dry zero grade air (BOC) was purged through the zero air generator and PTR-MS inlet in series to minimise instrument background and to prevent the build-up of contaminants. Immediately prior to take off, the sample flow was instantaneously switched to dry zero grade air contained in a 1 L silica coated stainless-steel can (Thames Restek, UK) within the aircraft, which was then continuously sampled until the aircraft had reached an altitude of 2500 m, allowing the PTR-MS to be fully operational during take-off.

VOC measurements were obtained at a sampling rate of 5 Hz and a repetition rate of ~ 2 Hz. The target protonated masses and likely contributing compounds were m/z 79 (benzene) and m/z 93 (toluene). Additionally, both the primary ion count m/z 21 ($\text{H}_3^{18}\text{O}^+$), its first water cluster ($\text{H}_3^{18}\text{O} \text{H}_2^{18}\text{O}^+$) at m/z 39 and O_2^+ at m/z 32 were determined. PTR-MS drift tube pressure, temperature and voltage were held constant at 2.0 mbar, 40 °C and 480 V respectively, maintaining an E/N ratio of approximately

**Airborne
determination of the
temporo-spatial
distribution**

M. D Shaw et al.

Title Page

Abstract

Introduction

Conclusions

References

Tables

Figures

◀

▶

◀

▶

Back

Close

Full Screen / Esc

Printer-friendly Version

Interactive Discussion

110 Td. For flights at ~ 360 m a.g.l., the m/z 21 primary ion count ranged between $(4-7) \times 10^7$ ion counts per second (cps) with an average of 6×10^7 . Ion counts of m/z 32 ranged between $(0.8-3) \times 10^6$ cps, with an average of 2×10^6 cps, which represented 3% of the primary ion signal. Ion counts of m/z 39 ranged between $(1-5) \times 10^6$ cps with an average of 3×10^6 cps, which represented 6% of the primary ion signal.

Toluene and benzene calibrations were carried out approximately 2 h prior to each flight using an in-house built dynamic dilution calibration system. This involved the dynamic dilution of a 500 ppbv certified gas standard (Apel, Riemer) with humidity controlled zero grade air (BOC gases) to mixing ratios near typically observed levels. Typical instrument sensitivities observed during the campaign ranged between 380–480 icps ppbv⁻¹, 6–8 normalised ion counts per second (ncps), and 400–600 icps ppbv⁻¹, 6–9 ncps, for benzene and toluene respectively. Instrument uncertainties were 16 ± 5 and 21 ± 9 % for benzene and toluene respectively, calculated using the standard deviation of linear regression (S_m) of pre-flight calibrations. Instrument limits of detection (LoDs) were determined by the method outlined by Taipale and colleagues (Taipale et al., 2008) and were 13 ± 8 and 18 ± 11 pptv for benzene and toluene respectively.

During flights, ambient air was sampled from the forward facing isokinetic inlet along a heated (70 °C) 5 m 1/4" Teflon (PFA) tube pumped by a stainless steel diaphragm pump (Millipore) at a flow-rate of 22 L min⁻¹. A portion of this ambient air (~ 300 sccm) was diverted into the pressure controlled inlet of the PTR-MS instrument such that the overall delay time was < 3 s. To determine blank VOC mixing ratios, the remaining ambient air was purged into a custom built zero air generator which consisted of a 3/8" stainless steel tube packed with 1 g of platinum coated quartz wool (Elemental Microanalysis) which efficiently removes VOCs (de Gouw et al., 2004). The zero air generator was operated at 350 °C and 30 psi for the duration of the flights to maintain optimal operating conditions. The catalytic converter does not remove water vapour from the sample stream, which is of particular importance as background impurities

may depend upon sample air humidity. During flights, zero air was periodically back-flushed through the inlet system to determine instrument background.

2.7 LAQN ground monitoring sites

Data were obtained from three LAQN ground level monitoring sites for comparative purposes. These were:

i. Marylebone Road (Westminster), an urban kerbside site in a street canyon, situated 1.5 m from the kerb of a frequently congested 6 lane road, the A501 (51.5225° N, 0.1546° W).

ii. Horseferry Road (Westminster), an urban background monitoring station located within an area of mixed commercial and residential buildings (51.4947° N, 0.1319° W). The nearest road is the B323 Horseferry Road approximately 17 m north of the station.

iii. Greenwich–Eltham (Eltham), a suburban background site situated in Greenwich within an education centre (51.4526° N, 0.0708° E). The site is approximately 25 m from the nearest road, the A210 Bexley Road. The surrounding area consists of trees, grass-land, recreational areas and suburban housing.

These sites all monitor NO, NO₂ and NO_x at hourly resolution and O₃ at 15 min resolution. However, only the Westminster–Marylebone Road and Greenwich–Eltham monitoring sites monitor benzene and toluene at hourly resolution. The locations are shown in Fig. S1 in the Supplement.

3 Results

3.1 Intercomparison of WAS TD-GCFID and PTR-MS

To compare the volume mixing ratios obtained with the on-board PTR-MS with those measured by gas chromatography with flame ionisation detection (GC-FID), whole air canister sampling (WAS) was conducted twice per flight using silica coated stainless steel cans (Thames Restek, UK) with subsequent GC-FID analysis for benzene and

Title Page

Abstract

Introduction

Conclusions

References

Tables

Figures



Back

Close

Full Screen / Esc

Printer-friendly Version

Interactive Discussion



Airborne determination of the temporo-spatial distribution

M. D Shaw et al.

Title Page

Abstract

Introduction

Conclusions

References

Tables

Figures



Back

Close

Full Screen / Esc

Printer-friendly Version

Interactive Discussion



toluene (Hopkins et al., 2009, 2003). The WAS system avoids possible artefact formation or analyte loss that may occur on adsorbents if a pre-concentration sampling system is used (Cao and Hewitt, 1993, 1994a, b). Previous ground observations in several urban environments have shown generally good agreement between benzene and toluene mixing ratios obtained during PTR-MS and GC-FID intercomparisons (Rogers et al., 2006; Warneke et al., 2001). However (Jobson et al., 2010) suggest a 16% overestimation of benzene mixing ratios determined by PTR-MS compared to a GC method, attributed to the fragmentation of higher alkyl-benzenes (eg ethyl-benzene). Inter-comparison of the two sampling methods showed excellent agreement within uncertainty and in particular suggest that the PTR-MS demonstrated minimal bias due to the fragmentation of higher alkyl benzenes during this study, as shown Fig. S2. Hence the PTR-MS signal obtained at m/z 79 is assumed to be due to benzene alone.

3.2 Interpretation of temporal trace gas profiles

Mixing ratios of VOCs, NO_x , O_3 and NO/NO_2 ratios from 27 individual flight-transects of Greater London during RF 2–6 were averaged to assess how they changed with respect to time over the 7 days of flights. As shown in Fig. 2, NO_x , benzene and toluene mixing ratios followed the typical diurnal pattern previously observed in urban areas with measured maxima during morning rush hours and a measured minimum at approximately 16:00–18:00 LT when O_3 reaches its maximum (Langford et al., 2010; Marr et al., 2013). The highest NO_x and VOC mixing ratios were observed in the morning at 10:30 LT, ~ 40 ppbv NO_x , ~ 350 pptv toluene and ~ 200 pptv benzene at 360 ± 10 m a.g.l., when emissions from traffic related sources are highest and the mixing height relatively low. Mixing ratios decreased throughout the morning, probably due to a combination of boundary layer development leading to dilution and increasing OH oxidation leading to enhanced chemical removal, with mixing ratios stabilising later in the day at 10–20 ppbv NO_x and between 90–150 pptv benzene and toluene. During the same period, O_3 mixing ratios were superficially anti-correlated to NO_x mixing ratios, increasing from morning minima until an evening maximum of 40–45 ppbv was

Airborne determination of the temporo-spatial distribution

M. D Shaw et al.

Title Page

Abstract

Introduction

Conclusions

References

Tables

Figures



Back

Close

Full Screen / Esc

Printer-friendly Version

Interactive Discussion



observed. Subsequently, the low O_3 morning and daytime mixing ratios over Greater London were attributed to the destruction of O_3 by rapid titration with NO . As the day progresses, sunlight intensity becomes higher increasing the NO_x oxidation rate leading to decreased NO_2 and increased O_3 (Pudasainee et al., 2010). Variations in O_3 mixing ratio are generally attributed to photochemical production in the mixing layer as well as transport from the upper layer (Dueñas et al., 2002).

Recent studies of annually averaged daily VOC mixing ratios in London from the 191 m high BT Tower have shown that benzene and toluene mixing ratios typically display two day-time maxima, one occurring around 9:00 LT and a second larger peak occurring between 18:00 and 21:00 LT coinciding with morning and evening peak traffic periods (Langford et al., 2010; Lee et al., 2014). NO_x mixing ratios are highest when traffic flow peaks, with higher O_3 mixing ratios corresponding to lower NO_x mixing ratios and vice versa during a 24 h period (Im et al., 2013; Lu and Wang, 2004; Mazzeo et al., 2005). This indicates that patterns in VOC and NO_x emission have a larger effect on observed mixing ratios in the boundary layer than does boundary layer dynamics.

3.3 Horizontal spatial distribution of VOCs and NO_x mixing ratios

The predominant wind directions observed during the flights were either north-westerly (RF 2–6), perpendicular to the flight transects, or north-easterly (RF 7–10), parallel to the flight transects (Table 1). Research flights 2–6 were used to provide a cross section of pollutant mixing ratios across London. The relative spatial distribution of VOC and NO_x mixing ratios across greater London during these flights were superficially consistent, with average mixing ratios for each flight leg only changing temporally (Fig. 2), hence only RF 5 is shown here.

Figures 3 and 4 show 1 km averaged mixing ratios of VOCs and NO_x respectively during RF 5 against latitude across Greater London. Both VOCs and NO_x mixing ratios show significantly higher mixing ratios in inner London. For all compounds the highest mixing ratios were observed within inner London at 360 ± 10 m a.g.l. particularly directly downwind of the London CCZ. Average mixing ratios observed within inner London

**Airborne
determination of the
temporo-spatial
distribution**

M. D Shaw et al.

Title Page

Abstract

Introduction

Conclusions

References

Tables

Figures



Back

Close

Full Screen / Esc

Printer-friendly Version

Interactive Discussion



were 0.20 ± 0.05 , 0.28 ± 0.07 , 13.2 ± 8.6 , 21.0 ± 7.3 and 34.3 ± 15.2 ppbv for benzene, toluene, NO, NO₂ and NO_x respectively. Mixing ratios for benzene, toluene, NO, NO₂ and NO_x for all flights are shown in Table 2.

Benzene, toluene and NO_x have shared anthropogenic sources with very few biogenic contributions in an urban environment. Vehicular emissions are considered to be an important source for VOCs and NO_x in Greater London (Langford et al., 2010; Lee et al., 2014). Toluene has a shorter atmospheric lifetime than benzene due to faster photochemical removal by OH (rate constants of $1.45 \pm 0.06 \times 10^{12} \text{ k}$, $\text{cm}^3 \text{ molecule}^{-1} \text{ s}^{-1}$; $6.03 \pm 0.17 \times 10^{12} \text{ k}$, $\text{cm}^3 \text{ molecule}^{-1} \text{ s}^{-1}$ for benzene and toluene respectively at 298 K; Ohta and Ohyama, 1985), thus the toluene to benzene (T/B) ratio can indicate the photochemical age of the pollution carried by air masses (Warneke et al., 2001; Atkinson, 2000). Very close to the source of emissions (e.g. at the kerbside), the ratio of VOC mixing ratios should be similar to those in the emissions themselves. As toluene is more rapidly removed by oxidation, the T/B ratio progressively decreases as air is transported over longer distances away from the source. Vehicular exhaust emission ratios from combustion during transient engine operation is dependent on gasoline composition but within Europe typically yield T/B ratios between $1.25\text{--}2.5 \text{ ppbv ppbv}^{-1}$ (Heeb et al., 2000). The introduction of catalytic converters to vehicular exhausts significantly has been shown to decrease this T/B ratio, attributed to the reduced catalytic conversion efficiency for benzene with respect to alkylated benzenes (Heeb et al., 2000). Hence observed ambient T/B mixing ratios will be a product of the photo-chemical age of the air mass since emission, vehicular fleet composition, gasoline composition and the ratio of vehicles using catalytic converters.

Recent long-term VOC measurements made at two ground level sites in central London (Marylebone Road and North Kensington; Valach et al., 2014) both dominated by traffic sources, showed T/B ratios of 1.6 ($1.3\text{--}2.0$) ppbv ppbv⁻¹ and 1.8 ($1.3\text{--}2.3$) ppbv ppbv⁻¹ respectively. These T/B ratios are similar to the average T/B concentration ratio of $1.8 \pm 0.3 \text{ ppbv ppbv}^{-1}$ observed within inner London in this study, where traffic sources are likely to be the highest (Fig. 4). Average T/B concentration ratios in

**Airborne
determination of the
temporo-spatial
distribution**

M. D Shaw et al.

Title Page

Abstract

Introduction

Conclusions

References

Tables

Figures

◀

▶

◀

▶

Back

Close

Full Screen / Esc

Printer-friendly Version

Interactive Discussion

suburban (latitude 51.30–51.35°) and south-western Greater London (latitude 51.35–51.42°) were 1.1 ± 0.3 ppbv ppbv⁻¹ and 1.3 ± 0.3 ppbv ppbv⁻¹ respectively. This could be interpreted as increasing air mass age from emission and suggests that the sources of benzene and toluene in these regions are likely the product of local emission and horizontal advection from inner London.

Linear regression analysis between NO, NO₂, NO_x, benzene and toluene mixing ratios yielded correlation coefficients (R^2) ranging between 0.12 and 0.64. The weakest linear regressions were observed between toluene and NO ($R^2 = 0.12$, $n = 7500$) and benzene and NO ($R^2 = 0.14$, $n = 6500$), not shown. The strongest linear regressions were observed between toluene and benzene ($R^2 = 0.51$, $n = 6500$) and toluene and NO₂ ($R^2 = 0.64$, $n = 7500$) (Fig. 5). This trimodal distribution between benzene, toluene and NO₂ indicates that these compounds potentially share the same or co-located sources within the Greater London area, most likely vehicular emission. However the measured NO₂/NO concentration ratio at 360 m a.g.l. is likely to be dominated by photochemistry rather than emission sources (Atkinson et al., 2000).

Figure 5 also suggests a secondary source contribution to toluene that is not shared with NO₂ or benzene and hence is not related to traffic emissions. This secondary source is localised to a discrete peak in observed toluene in SE London within the borough of Lambeth (latitude 51.455°, longitude -0.141°). This was observed during three of the seven flight transects in which toluene mixing ratios at 360 ± 10 m a.g.l. increased from 0.25 to 0.6 ppbv with a T/B ratio of up to 3 ppbv ppbv⁻¹, as seen in Fig. 3. Toluene has numerous anthropogenic sources including evaporative fuel losses, industrial solvents, paint thinners and the manufacturing of ink and paints. Direct toluene emissions from industrialised areas in Mexico city with T/B ratios of up to 8.5–12.5 ppbv ppbv⁻¹ have previously been reported (Karl et al., 2009). In the absence of any identifiable industrialised areas upwind of the region of high T/B ratios in Lambeth, this peak is possibly due to the horizontal advection of industrial emissions from outside of London, or some unidentified localised source of toluene.

Airborne determination of the temporo-spatial distribution

M. D Shaw et al.

Title Page

Abstract

Introduction

Conclusions

References

Tables

Figures

◀

▶

◀

▶

Back

Close

Full Screen / Esc

Printer-friendly Version

Interactive Discussion

The influence of NO_x and VOC emission from London Heathrow Airport (LHA) during this study was investigated with plume dispersion modelling using the NOAA Hybrid Single-Particle Lagrangian Integrated Trajectory (HYSPPLIT) model. The model isolates the region of the flight track influenced by potential pollutant outflow from LHA during the flight. Four hour averaged forward dispersion forecasting was modelled for RF5 from LHA between 9 a.m.–12 p.m. LT. The lower and upper limits of the averaged dispersion layer were 300–400 m a.g.l., similar to the measured average flight altitude of 366 ± 7.2 m a.g.l. during RF 5. During RF 5 the transport time from LHA to the flight transect was approximately 50 min, calculated from the average observed horizontal wind speed and the ~ 20 km downwind distance (Fig. 7).

Figure 6 shows the region of RF 5 flight transects which were influenced by LHA outflow ($51.39\text{--}51.45^\circ$ latitude). On entering the LHA outflow plume, NO_x mixing ratios at 360 ± 10 m a.g.l. were observed to increase from 18 to 30 ppbv, suggesting a strong NO_x source. As shown in Fig. 4, the NO/NO_2 ratio also gradually increased across the plume from 0.5 up to $0.8 \text{ ppbv ppbv}^{-1}$, which is consistent with previous studies that have found higher NO mixing ratios in aircraft exhaust (Spicer et al., 1994; Schäfer et al., 2000). Toluene and benzene mixing ratios showed a negligible increase from 0.20–0.26 and 0.15–0.18 ppbv at 360 ± 10 m a.g.l. across the plume respectively, with T/B ratios of $1.5\text{--}1.7 \text{ ppbv ppbv}^{-1}$ indicative of vehicular exhaust emission as the dominant VOC source. Previous ground observations (Carslaw et al., 2006) at LHA suggested that approximately 27 % of the annual mean NO_x and NO_2 were due to airport operations at the airport boundary. At background locations 2–3 km downwind of the airport they estimated that the upper limit of the airport contribution to be less than 15 %. Our measurements are in qualitative agreement with this study, suggesting that even though Heathrow is an important emission source of NO_x , observed mixing ratios of NO_x close to the airport are dominated by road traffic sources. As LHA was ~ 20 km upwind of the flight transects, our observed mixing ratios are likely to be heavily influenced by emissions during advection from LHA to the measurement location and local sources within inner London and as such conclusions drawn from this data is tentative.

Airborne determination of the temporo-spatial distribution

M. D Shaw et al.

Title Page

Abstract

Introduction

Conclusions

References

Tables

Figures

⏪

⏩

⏴

⏵

Back

Close

Full Screen / Esc

Printer-friendly Version

Interactive Discussion



VOC and NO_x emissions from airports are due to a combination of emissions from aircraft exhaust, ground support equipment (GSE) exhaust and evaporative losses during aircraft refuelling. High mixing ratios of aromatic compounds, such as toluene and benzene, and low NO_x mixing ratios have been previously observed in jet engine exhaust immediately after ignition, attributed to low engine temperature causing incomplete combustion (Schürmann et al., 2007). Previous aircraft exhaust studies have shown T/B ratios observed during engine ignition are up to 3.1 ppbv ppbv⁻¹, typical of kerosene fuel. At higher engine temperatures, i.e. during taxiing, higher aromatics tend to crack leading to a reduced amount of these species, but increasing amounts of benzene. Thus for aircraft taxiing, a T/B ratio of ~ 0.5 ppbv ppbv⁻¹ was previously observed (Spicer et al., 1985). Similarly higher NO_x mixing ratios are observed due to higher engine combustion. As well as the contribution from aircraft, additional emissions from airport environments occur during the handling of aircraft with GSE. The GSE vehicles are mostly diesel powered, leading to relatively high emission rates of the oxides of nitrogen. During aircraft refuelling, gaseous air-fuel mixtures are released from the aircraft tanks through fuel vents which can be discriminated by the observed T/B ratio, since kerosene fuel tends to have an enhanced amount of aromatic compounds. VOC emissions during engine refuelling were previously found to account for 2.7 % of the total VOC emissions of Zurich airport (Schürmann et al., 2007).

3.4 Interpretation of vertical trace gas profiles

To date the influence of vertical transport on the distribution of trace gases in the urban boundary layer has primarily been studied with respect to vertical profiles of ozone, which are typically with in-situ instruments mounted on tethered balloons (Beyrich et al., 1996; Güsten et al., 1998; Newchurch et al., 2003). Vertical profiling of VOCs, NO, NO₂ and NO_x have also been studied using a combination of in-situ measurements from tethered balloons and ground based differential optical absorption spectroscopy (DOAS) over several American (Wang et al., 2003; Stutz et al., 2004; Velasco et al., 2008; Hu et al., 2012) and European cities (Glaser et al., 2003). To the author's knowl-

Airborne determination of the temporo-spatial distribution

M. D Shaw et al.

Title Page

Abstract

Introduction

Conclusions

References

Tables

Figures



Back

Close

Full Screen / Esc

Printer-friendly Version

Interactive Discussion



the kerbside site, 17 ppb, increasing to 32 ppbv at 360 ± 10 m a.g.l. The daytime vertical profiles of NO, NO₂ and O₃ are caused due to a combination of turbulent mixing and three main simultaneous competing effects. The chemical production of NO₂ by NO titration with O₃ and RO₂, causing higher NO₂ and lower O₃ mixing ratios closer to the surface due to higher surface NO mixing ratios. Photochemical production of NO and O₃ from NO₂ and subsequent O₃ destruction. NO₂ and ozone dry deposition processes which dominate closer to the surface (Wesely and Hicks, 2000).

The vertical profiles of NO_x and O₃ are superficially anti-correlated with altitude. The observed O₃ profiles, with lower values close to the ground and higher values aloft, agree in their general behaviour with other observations (Beyrich et al., 1996; Glaser et al., 2003; Güsten et al., 1998) The vertical profiles of O₃ and O_x (the sum of O₃ and NO₂) show the importance of NO emission for O₃ depletion, with reduced surface O₃ mixing ratios closer to the ground largely compensated by a corresponding increase in NO₂. As a result, O_x exhibits a very uniform vertical concentration between 350–650 m a.g.l. However, O_x mixing ratios are substantially reduced at ground level likely due to enhanced O₃ titration with NO, associated with the proximity of the Marylebone road site to the vehicular emission source.

3.5 Comparison of airborne measurements with LAQN ground sites

Data obtained from three LAQN air quality ground monitoring stations located in three typical urban environments (urban kerbside: Marylebone Road; urban background: Westminster–Horseferry Road; and suburban background: Greenwich–Eltham) were compared against airborne mixing ratios at 360 ± 10 m a.g.l. to assess how O₃ and its precursors are distributed across the city. Dispersion modelling using the NOAA HYSPLIT model was used to highlight regions of the flight track most influenced by pollutant outflow from each of the ground monitoring stations. Briefly, four hour averaged forward and reverse dispersion forecasting was modelled for Marylebone Road, Westminster and Eltham respectively during flights with a prevailing north westerly wind direction (RF 1, RF4–6, Table 1). RF 2 and 3 were not used in the comparison due

**Airborne
determination of the
temporo-spatial
distribution**

M. D Shaw et al.

[Title Page](#)[Abstract](#)[Introduction](#)[Conclusions](#)[References](#)[Tables](#)[Figures](#)[Back](#)[Close](#)[Full Screen / Esc](#)[Printer-friendly Version](#)[Interactive Discussion](#)

to low observed wind speeds, $< 5 \text{ m s}^{-1}$. The lower and upper limits of the averaged dispersion layer were 300–400 m a.g.l., similar to the measured average flight altitude of $360 \pm 10 \text{ m a.g.l.}$ during RF 1, RF4–6. Airborne mixing ratios for comparison were given as the arithmetic average and 1 SD of the hourly measurements within the dispersion plume. The approximate transport times from Marylebone Road, Westminster and Eltham to the flight transect ranged between 3–7, 7–15 and 14–28 min respectively, calculated from the observed horizontal wind speed and the downwind/upwind distance for each ground station during each flight (Fig. S1).

Figure 8 shows a linear regression analysis between airborne and ground mixing ratios of benzene, toluene, NO, NO₂, NO_x and O₃. Strong positive correlations are observed for all species at all three ground sites with R^2 values ranging from 0.54–0.97 ($n = 7$). Ground mixing ratios of both VOCs and NO_x species were significantly higher at the Marylebone Road kerbside site relative to the urban background (Westminster) and suburban background (Eltham) sites. Average mixing ratios observed at ground level for benzene and toluene respectively were 0.12 ± 0.05 ; 0.21 ± 0.08 ppbv at Marylebone Road and 0.07 ± 0.01 ; 0.13 ± 0.03 ppbv at Eltham, with T/B ratios of 1.7–1.8 ppbv ppbv⁻¹ indicative of vehicular emissions as the dominant source at both sites. NO_x mixing ratios were also significantly higher at Marylebone Road (121.96 ± 45.28 ppbv) than Westminster (40 ± 4.45 ppbv) and Eltham (10.02 ± 4.28). For O₃, the mean mixing ratios observed at Westminster (13.56 ± 4.9 ppbv) were lower than at Eltham (19.14 ± 3.2 ppbv) whilst the lowest mixing ratios were at the Marylebone Road site (9.23 ± 8.42 ppbv). The O₃ mixing ratios at these sites are anti-correlated to that of NO (Fig. 8), through enhanced NO emission and subsequent titration of O₃ in proximity to busy road networks.

Also of interest, NO/NO₂ ratios were higher at the Marylebone Road site (0.62 ± 0.25) than at Westminster (0.50 ± 0.15) and Eltham (0.25 ± 0.09). Historically, vehicular diesel and petrol emissions of NO_x were dominated by emissions of NO (NO/NO₂ ratios of (NO / NO₂ ratios of ≤ 0.9)). However, recent developments in diesel emission technology, specifically diesel oxidation catalysts and particulate filters, have

**Airborne
determination of the
temporo-spatial
distribution**

M. D Shaw et al.

[Title Page](#)[Abstract](#)[Introduction](#)[Conclusions](#)[References](#)[Tables](#)[Figures](#)[Back](#)[Close](#)[Full Screen / Esc](#)[Printer-friendly Version](#)[Interactive Discussion](#)

caused significant increases in direct vehicular NO_2 emissions in the UK and Europe. Current diesel emission control technology deliberately produces enhanced NO_2 mixing ratios to oxidise and reduce black carbon particulates in the vehicular exhaust gas (Carslaw and Rhys-Tyler, 2013). Increasing numbers of diesel vehicles in Central London with this emission reduction technology could have contributed to the low NO/NO_2 ratios observed from all three ground air monitoring stations observed during this study. This is in good agreement with the trimodal distribution of benzene, toluene and NO_2 shown in Fig. 5, potentially indicating these species have common sources, most likely from vehicular emission. However the measured NO/NO_2 concentration ratio at 360 m a.g.l. is likely to be dominated by photochemistry rather than emission sources (Atkinson et al., 2000).

Airborne mixing ratios of O_3 were consistently higher than those at ground level, consistent with the ground surface in London acting as a chemical sink for O_3 , which is in good agreement with the measured vertical profile of O_3 shown in Fig. 7. Mixing ratios of the selective VOC and NO_x species observed at the roadside site at Marylebone Road were significantly higher than those of the airborne measurements. Assuming this difference is due entirely to mixing, this reduction in mixing ratio crudely indicates a dilution factor of 2–6 between the roadside site in the Marylebone Road and the 355 m sampling point. This agrees well with comparisons made during REPARTÉE I which concluded a dilution factor of ~ 5 for NO_x mixing ratios between Marylebone Road and the 190 m sampling point on the BT tower (Harrison et al., 2012), well above the surrounding building height. Dilution factors for VOC and NO_x species at Westminster and Eltham ranged between 0.46–2.34 which are significantly lower than those observed at Marylebone Road. This difference in dilution factors is largely due to firstly the Marylebone Road measurement site being in central London, a very large source of VOCs and NO_x and being closest in proximity to the 6 lane frequently congested road. Secondly Marylebone Road is within an urban street canyon whose orientation serves to maximise mixing ratios of emissions therein. Street canyons are not as well ventilated as with more open locations such as urban and suburban sites which tends

to result in increased surface mixing ratios (Pugh et al., 2012; Carslaw and Rhys-Tyler, 2013).

4 Conclusions

Measurements of VOCs, NO_x and O_3 in the boundary layer were made in transects across Greater London at 360 ± 10 m a.g.l. during the summer of 2013, with a view to identifying the dominant O_3 precursor sources within the region, and to better understanding the effects of chemical interactions between these pollutants and meteorological variables on urban air quality. Observed benzene, toluene and NO_x mixing ratios across Greater London were mostly due to traffic emissions, with the highest mixing ratios observed over inner London, where the density of traffic and other pollutant sources is higher than over outer London. The highest T/B ratios (1.8 ± 0.3 ppbv ppbv⁻¹) observed within inner London is indicative of local vehicular sources. Linear regression analysis of VOC and NO_x species which showed a trimodal correlation between benzene, toluene and NO_2 , potentially indicating that their dominant sources are the same or are co-located throughout London. The reason these VOCs correlate well with NO_2 , but not NO is possibly because of the ubiquity of diesel vehicles in London. Modern diesel vehicles use emission control technology to reduce black carbon emissions but which also enhance the NO_2/NO ratio in the vehicle exhaust (Carslaw and Rhys-Tyler, 2013). However the measured NO_2/NO concentration ratio at 360 m a.g.l. is likely to be dominated by photochemistry rather than emission sources (Atkinson et al., 2000).

Airborne mixing ratios were compared to kerbside data from three LAQN air quality ground monitoring stations within Greater London. Strong positive correlations were observed for O_3 , NO , NO_2 , NO_x , benzene and toluene species at all three ground sites with R^2 values ranging from 0.54–0.97 ($n = 7$) suggesting that airborne mixing ratios were characteristic of surface mixing ratios during the analysis period. NO_x and VOC mixing ratios observed at the Marylebone Road air quality monitoring site were 2–6 times higher than those observed at 360 ± 10 m a.g.l. agl due to a combination of its

Airborne determination of the temporo-spatial distribution

M. D Shaw et al.

Title Page

Abstract

Introduction

Conclusions

References

Tables

Figures



Back

Close

Full Screen / Esc

Printer-friendly Version

Interactive Discussion



proximity to the emission sources, photochemical aging and dilution of the air mass during vertical mixing.

An increase in NO_x mixing ratios from 18 to 30 ppbv at 360 ± 10 m a.g.l. was observed ~ 20 km downwind of LHA. Our measurements tentatively support previous studies that suggest that even though Heathrow is an important emission source of NO_x, observed mixing ratios of NO_x even quite close to the airport are dominated by road traffic sources. Since LHA was ~ 20 km upwind of the flight transects, these observed mixing ratios are likely to be heavily influenced by vehicular emissions during advection from LHA to the measurement location.

The Supplement related to this article is available online at doi:10.5194/acpd-14-27335-2014-supplement.

Author contributions. M. D. Shaw and J. D. Lee redesigned the PTR-MS and NO_x chemiluminescence instruments for the aircraft. M. D. Shaw, J. D. Lee and B. Davison designed the field experiment and carried it out. M. D. Shaw, J. D. Lee, A. Vaughan, R. M. Purvis, A. C. Lewis and C. N. Hewitt were responsible for analysis/interpretation of the data.

Acknowledgements. We thank the UK Natural Environment Research Council (grant NE/J00779X/1) and the Department of Environment, Food and Rural Affairs for funding. We thank Captain Carl Joseph, co-pilot James Johnson and instrumental engineer Thomas Millard (ARSF) for their expert support during the flights and James Hopkins and Shallini Punjabi (National Centre for Atmospheric Science, University of York, UK) for the WAS TD-GC-FID benzene and toluene concentration data.

References

Atkinson, R.: Atmospheric chemistry of VOCs and NO_x, *Atmos. Environ.*, 34, 2063–2101, 2000.
Beswick, K. M., Gallagher, M. W., Webb, A. R., Norton, E. G., and Perry, F.: Application of the Aventech AIMMS20AQ airborne probe for turbulence measurements during the Convective

27356

ACPD

14, 27335–27371, 2014

Airborne determination of the temporo-spatial distribution

M. D Shaw et al.

Title Page

Abstract

Introduction

Conclusions

References

Tables

Figures



Back

Close

Full Screen / Esc

Printer-friendly Version

Interactive Discussion



**Airborne
determination of the
temporo-spatial
distribution**

M. D Shaw et al.

Title Page

Abstract

Introduction

Conclusions

References

Tables

Figures

◀

▶

◀

▶

Back

Close

Full Screen / Esc

Printer-friendly Version

Interactive Discussion



Storm Initiation Project, Atmos. Chem. Phys., 8, 5449–5463, doi:10.5194/acp-8-5449-2008, 2008.

Beyrich, F., Weisensee, U., Sprung, D., and Güsten, H.: Comparative analysis of sodar and ozone profile measurements in a complex structured boundary layer and implications for mixing height estimation, Bound.-Lay. Meteorol., 81, 1–9, 1996.

Cao, X.-L. and Hewitt, C. N.: Thermal desorption efficiencies for different adsorbate/adsorbent systems typically used in air monitoring programmes, Chemosphere, 27, 695–705, 1993.

Cao, X.-L. and Hewitt, C. N.: Study of the degradation by ozone of adsorbents and of hydrocarbons adsorbed during the passive sampling of air, Environ. Sci. Technol., 28, 757–762, 1994a.

Cao, X.-L. and Hewitt, C. N.: Build-up of artifacts on adsorbents during storage and its effect on passive sampling and gas chromatography-flame ionization detection of low concentrations of volatile organic compounds in air, J. Chromatogr. A, 688, 368–374, 1994b.

Carslaw, D. C. and Rhys-Tyler, G.: New insights from comprehensive on-road measurements of NO_x, NO₂ and NH₃ from vehicle emission remote sensing in London, UK, Atmos. Environ., 81, 339–347, 2013.

Carslaw, D. C., Beevers, S. D., Ropkins, K., and Bell, M. C.: Detecting and quantifying aircraft and other on-airport contributions to ambient nitrogen oxides in the vicinity of a large international airport, Atmos. Environ., 40, 5424–5434, 2006.

de Gouw, J. and Warneke, C.: Measurements of volatile organic compounds in the earth's atmosphere using proton-transfer-reaction mass spectrometry, Mass Spectrom. Rev., 26, 223–257, 2007.

de Gouw, J., Warneke, C., Holzinger, R., Klüpfel, T., and Williams, J.: Inter-comparison between airborne measurements of methanol, acetonitrile and acetone using two differently configured PTR-MS instruments, Int. J. Mass Spectrom., 239, 129–137, 2004.

Dueñas, C., Fernández, M., Cañete, S., Carretero, J., and Liger, E.: Assessment of ozone variations and meteorological effects in an urban area in the Mediterranean Coast, Sci. Total Environ., 299, 97–113, 2002.

Glaser, K., Vogt, U., Baumbach, G., Volz-Thomas, A., and Geiss, H.: Vertical profiles of O₃, NO₂, NO_x, VOC, and meteorological parameters during the Berlin Ozone Experiment (BERLIOZ) campaign, J. Geophys. Res.-Atmos., 108, 8253, doi:10.1029/2002JD002475, 2003.

**Airborne
determination of the
temporo-spatial
distribution**

M. D Shaw et al.

Title Page

Abstract

Introduction

Conclusions

References

Tables

Figures



Back

Close

Full Screen / Esc

Printer-friendly Version

Interactive Discussion



- Güsten, H., Heinrich, G., and Sprung, D.: Nocturnal depletion of ozone in the Upper Rhine Valley, *Atmos. Environ.*, 32, 1195–1202, 1998.
- Harrison, R. M., Dall'Osto, M., Beddows, D. C. S., Thorpe, A. J., Bloss, W. J., Allan, J. D., Coe, H., Dorsey, J. R., Gallagher, M., Martin, C., Whitehead, J., Williams, P. I., Jones, R. L., Langridge, J. M., Benton, A. K., Ball, S. M., Langford, B., Hewitt, C. N., Davison, B., Martin, D., Petersson, K. F., Henshaw, S. J., White, I. R., Shallcross, D. E., Barlow, J. F., Dunbar, T., Davies, F., Nemitz, E., Phillips, G. J., Helfter, C., Di Marco, C. F., and Smith, S.: Atmospheric chemistry and physics in the atmosphere of a developed megacity (London): an overview of the REPARTEE experiment and its conclusions, *Atmos. Chem. Phys.*, 12, 3065–3114, doi:10.5194/acp-12-3065-2012, 2012.
- Hayward, S., Hewitt, C., Sartin, J., and Owen, S.: Performance characteristics and applications of a proton transfer reaction-mass spectrometer for measuring volatile organic compounds in ambient air, *Environ. Sci. Technol.*, 36, 1554–1560, 2002.
- Heeb, N. V., Forss, A.-M., Bach, C., Reimann, S., Herzog, A., and Jäckle, H. W.: A comparison of benzene, toluene and C2-benzenes mixing ratios in automotive exhaust and in the suburban atmosphere during the introduction of catalytic converter technology to the Swiss Car Fleet, *Atmos. Environ.*, 34, 3103–3116, 2000.
- Hewitt, C., Hayward, S., and Tani, A.: The application of proton transfer reaction-mass spectrometry (PTR-MS) to the monitoring and analysis of volatile organic compounds in the atmosphere, *J. Environ. Monitor.*, 5, 1–7, 2003.
- Hopkins, J. R., Lewis, A. C., and Read, K. A.: A two-column method for long-term monitoring of non-methane hydrocarbons (NMHCs) and oxygenated volatile organic compounds (o-VOCs), *J. Environ. Monitor.*, 5, 8–13, 2003.
- Hopkins, J. R., Evans, M. J., Lee, J. D., Lewis, A. C., H Marsham, J., McQuaid, J. B., Parker, D. J., Stewart, D. J., Reeves, C. E., and Purvis, R. M.: Direct estimates of emissions from the megacity of Lagos, *Atmos. Chem. Phys.*, 9, 8471–8477, doi:10.5194/acp-9-8471-2009, 2009.
- Hu, S., Paulson, S. E., Fruin, S., Kozawa, K., Mara, S., and Winer, A. M.: Observation of elevated air pollutant concentrations in a residential neighborhood of Los Angeles California using a mobile platform, *Atmos. Environ.*, 51, 311–319, 2012.
- Im, U., Incecik, S., Guler, M., Tek, A., Topcu, S., Unal, Y. S., Yenigun, O., Kindap, T., Odman, M. T., and Tayanc, M.: Analysis of surface ozone and nitrogen oxides at urban, semi-rural and rural sites in Istanbul, Turkey, *Sci. Total Environ.*, 443, 920–931, 2013.

**Airborne
determination of the
temporo-spatial
distribution**

M. D Shaw et al.

Title Page

Abstract

Introduction

Conclusions

References

Tables

Figures



Back

Close

Full Screen / Esc

Printer-friendly Version

Interactive Discussion



- Jobson, B. T., Volkamer, R. A., Velasco, E., Allwine, G., Westberg, H., Lamb, B. K., Alexander, M. L., Berkowitz, C. M., and Molina, L. T.: Comparison of aromatic hydrocarbon measurements made by PTR-MS, DOAS and GC-FID during the MCMA 2003 Field Experiment, *Atmos. Chem. Phys.*, 10, 1989–2005, doi:10.5194/acp-10-1989-2010, 2010.
- 5 Kansal, A.: Sources and reactivity of NMHCs and VOCs in the atmosphere: a review, *J. Hazard. Mater.*, 166, 17–26, 2009.
- Karl, T., Apel, E., Hodzic, A., Riemer, D. D., Blake, D. R., and Wiedinmyer, C.: Emissions of volatile organic compounds inferred from airborne flux measurements over a megacity, *Atmos. Chem. Phys.*, 9, 271–285, doi:10.5194/acp-9-271-2009, 2009.
- 10 Langford, B., Nemitz, E., House, E., Phillips, G. J., Famulari, D., Davison, B., Hopkins, J. R., Lewis, A. C., and Hewitt, C. N.: Fluxes and concentrations of volatile organic compounds above central London, UK, *Atmos. Chem. Phys.*, 10, 627–645, doi:10.5194/acp-10-627-2010, 2010.
- Lee, J., Moller, S., Read, K., Lewis, A., Mendes, L., and Carpenter, L.: Year-round measurements of nitrogen oxides and ozone in the tropical North Atlantic marine boundary layer, *J. Geophys. Res.*, 114, D21302, doi:10.1029/2009JD011878, 2009.
- Lee, J., Helfter, C., Purvis, R., Beavers, S., Carslaw, D., Lewis, A., Moller, S., Nemitz, E., and Tremper, A.: Measurement NO_x fluxes from a tall tower above central London, UK and comparison with emissions inventories., *Environ. Sci. Technol.*, under review, 2014.
- 20 Lu, W. and Wang, X.: Interaction patterns of major air pollutants in Hong Kong territory, *Sci. Total Environ.*, 324, 247–259, 2004.
- Marr, L. C., Moore, T. O., Klapmeyer, M. E., and Killar, M. B.: Comparison of NO_x fluxes measured by eddy covariance to emission inventories and land use, *Environ. Sci. Technol.*, 47, 1800–1808, doi:10.1021/es303150y, 2013.
- 25 Mazzeo, N. A., Venegas, L. E., and Choren, H.: Analysis of NO , NO_2 , O_3 and NO_x concentrations measured at a green area of Buenos Aires City during wintertime, *Atmos. Environ.*, 39, 3055–3068, 2005.
- Na, K., Moon, K.-C., and Kim, Y. P.: Source contribution to aromatic VOC concentration and ozone formation potential in the atmosphere of Seoul, *Atmos. Environ.*, 39, 5517–5524, 2005.
- 30 Nelson, P., Quigley, S., and Smith, M.: Sources of atmospheric hydrocarbons in Sydney: a quantitative determination using a source reconciliation technique, *Atmos. Environ.*, 17, 439–449, 1983.

**Airborne
determination of the
temporo-spatial
distribution**

M. D Shaw et al.

Title Page

Abstract

Introduction

Conclusions

References

Tables

Figures



Back

Close

Full Screen / Esc

Printer-friendly Version

Interactive Discussion



Newchurch, M., Ayoub, M., Oltmans, S., Johnson, B., and Schmidlin, F.: Vertical distribution of ozone at four sites in the United States, *J. Geophys. Res.-Atmos.*, 108, ACH 9-1–ACH 9-17, 2003.

Ohta, T. and Ohyama, T.: A set of rate constants for the reactions of OH radicals with aromatic hydrocarbons, *B. Chem. Soc. Jpn.*, 58, 3029–3030, 1985.

Pollack, I. B., Lerner, B. M., and Ryerson, T. B.: Evaluation of ultraviolet light-emitting diodes for detection of atmospheric NO₂ by photolysis-chemiluminescence, *J. Atmos. Chem.*, 65, 111–125, 2010.

Pudasainee, D., Sapkota, B., Bhatnagar, A., Kim, S.-H., and Seo, Y.-C.: Influence of weekdays, weekends and bandhas on surface ozone in Kathmandu valley, *Atmos. Res.*, 95, 150–156, 2010.

Pugh, T. A., MacKenzie, A. R., Whyatt, J. D., and Hewitt, C. N.: Effectiveness of green infrastructure for improvement of air quality in urban street canyons, *Environ. Sci. Technol.*, 46, 7692–7699, 2012.

Rogers, T., Grimsrud, E., Herndon, S., Jayne, J., Kolb, C. E., Allwine, E., Westberg, H., Lamb, B., Zavala, M., and Molina, L.: On-road measurements of volatile organic compounds in the Mexico City metropolitan area using proton transfer reaction mass spectrometry, *Int. J. Mass Spectrom.*, 252, 26–37, 2006.

Schäfer, K., Heland, J., Lister, D. H., Wilson, C. W., Howes, R. J., Falk, R. S., Lindermeir, E., Birk, M., Wagner, G., and Haschberger, P.: Nonintrusive optical measurements of aircraft engine exhaust emissions and comparison with standard intrusive techniques, *Appl. Optics*, 39, 441–455, 2000.

Schürmann, G., Schäfer, K., Jahn, C., Hoffmann, H., Bauerfeind, M., Fleuti, E., and Rappenglück, B.: The impact of NO, CO and VOC emissions on the air quality of Zurich airport, *Atmos. Environ.*, 41, 103–118, 2007.

Spicer, C. W., Holdren, M. W., Riggan, R. M., and Lyon, T. F.: Chemical composition and photochemical reactivity of exhaust from aircraft turbine engines, *Ann. Geophys.*, 12, 944–955, doi:10.1007/s00585-994-0944-0, 1994.

Stutz, J., Alicke, B., Ackermann, R., Geyer, A., White, A., and Williams, E.: Vertical profiles of NO₃, N₂O₅, O₃, and NO_x in the nocturnal boundary layer: 1. observations during the Texas Air Quality Study 2000, *J. Geophys. Res.-Atmos.*, 109, D12306, doi:10.1029/2003JD004209, 2004.

**Airborne
determination of the
temporo-spatial
distribution**

M. D Shaw et al.

Title Page

Abstract

Introduction

Conclusions

References

Tables

Figures



Back

Close

Full Screen / Esc

Printer-friendly Version

Interactive Discussion



Taipale, R., Ruuskanen, T. M., Rinne, J., Kajos, M. K., Hakola, H., Pohja, T., and Kulmala, M.: Technical note: Quantitative long-term measurements of VOC concentrations by PTR-MS – measurement, calibration, and volume mixing ratio calculation methods, *Atmos. Chem. Phys.*, 8, 6681–6698, doi:10.5194/acp-8-6681-2008, 2008.

5 Valach, A., Langford, B., Nemitz, E., MacKenzie, A., and Hewitt, C.: Concentrations of selected volatile organic compounds at kerbside and background sites in central London, *Atmos. Environ.*, 95, 456–467, doi:10.1016/j.atmosenv.2014.06.052, 2014.

Velasco, E., Márquez, C., Bueno, E., Bernabé, R. M., Sánchez, A., Fentanes, O., Wöhrnschimmel, H., Cárdenas, B., Kamilla, A., Wakamatsu, S., and Molina, L. T.: Vertical distribution of ozone and VOCs in the low boundary layer of Mexico City, *Atmos. Chem. Phys.*, 8, 3061–3079, doi:10.5194/acp-8-3061-2008, 2008.

10 Wang, S., Ackermann, R., Geyer, A., Doran, J. C., Shaw, W. J., Fast, J. D., Spicer, C. W., and Stutz, J.: Vertical variation of nocturnal NO_x chemistry in the urban environment of Phoenix, in: *Extended Abstracts, Fifth Conference on Atmospheric Chemistry in the 83rd AMS Annual Meeting*, CD-ROM, P1.1, Am. Meteorol. Soc., Long Beach, CA, 2003.

15 Warneke, C., Van der Veen, C., Luxembourg, S., De Gouw, J., and Kok, A.: Measurements of benzene and toluene in ambient air using proton-transfer-reaction mass spectrometry: calibration, humidity dependence, and field intercomparison, *Int. J. Mass Spectrom.*, 207, 167–182, 2001.

20 Watson, J. G., Chow, J. C., and Fujita, E. M.: Review of volatile organic compound source apportionment by chemical mass balance, *Atmos. Environ.*, 35, 1567–1584, 2001.

Wesely, M. and Hicks, B.: A review of the current status of knowledge on dry deposition, *Atmos. Environ.*, 34, 2261–2282, 2000.

Airborne determination of the temporo-spatial distribution

M. D Shaw et al.

Title Page

Abstract

Introduction

Conclusions

References

Tables

Figures

◀

▶

◀

▶

Back

Close

Full Screen / Esc

Printer-friendly Version

Interactive Discussion



Table 1. Summary of meteorological and flight conditions during campaign.

RF	Date	Time (local)	Mean Wind direction (°)	Mean Wind speed (m s ⁻¹)	Mean True airspeed (m s ⁻¹)	Mean Flight altitude a.g.l. (m)
1	24 Jun 13	15:30–18:20	285.9 ± 17.1	13.6 ± 3.3	81.1 ± 3.9	603 ± 28.9
2	26 Apr 13	16:00–18:00	287.5 ± 17.0	5.8 ± 1.0	70.7 ± 3.4	349.8 ± 15.1
3	27 Jun 13	9:40–12:15	277.6 ± 20.9	4.2 ± 1.4	69.6 ± 2.7	354.1 ± 11.1
4	27 Jun 13	14:20–17:50	275.1 ± 24.5	6.6 ± 1.6	72.6 ± 5.4	343.1 ± 31.7
5	3 Jul 13	10:40–13:00	280.7 ± 11.0	6.3 ± 1.3	71.9 ± 4.0	366.1 ± 7.2
6	4 Jul 13	15:20–16:55	240.7 ± 11.3	7.5 ± 1.4	72.5 ± 4.5	365.1 ± 18.3
7	8 Jul 13	11:30–13:00	56.4 ± 13.3	7.3 ± 1.4	70.5 ± 4.9	354 ± 13.6
8	8 Jul 13	16:30–18:00	54.3 ± 16.9	7.4 ± 1.4	77.5 ± 3.1	361 ± 8.7
9	9 Jul 13	9:30–11:30	52.1 ± 44.5	5.3 ± 1.4	75.7 ± 5.2	376 ± 28.8
10	9 Jul 13	14:00–16:00	52.8 ± 35.6	5.6 ± 1.3	76.6 ± 6.7	355.4 ± 14.8

Airborne determination of the temporo-spatial distribution

M. D Shaw et al.

[Title Page](#)
[Abstract](#)
[Introduction](#)
[Conclusions](#)
[References](#)
[Tables](#)
[Figures](#)

[Back](#)
[Close](#)
[Full Screen / Esc](#)
[Printer-friendly Version](#)
[Interactive Discussion](#)


Table 2. Summary of mixing ratios (ppbv) observed over inner London during campaign.

	RF1	RF2	RF3	RF4	RF5	RF6	RF7	RF8	RF9	RF10
Benzene										
Mean	0.08	0.09	0.22	0.10	0.20	0.10	0.17	0.18	0.10	0.07
Median	0.07	0.09	0.15	0.09	0.19	0.10	0.17	0.18	0.09	0.07
SD	0.06	0.05	0.06	0.05	0.05	0.05	0.05	0.07	0.08	0.05
5th percentile	0.01	0.03	0.06	0.03	0.09	0.03	0.09	0.08	0.01	0.01
95th percentile	0.178	0.20	0.27	0.17	0.22	0.19	0.26	0.30	0.25	0.16
<i>N</i>	16 500	13 900	14 100	2560	7620	11 260	8860	8950	12 600	12 100
Toluene										
Mean	0.17	0.12	0.28	0.15	0.28	0.12	0.20	0.14	0.29	0.14
Median	0.16	0.12	0.27	0.15	0.25	0.11	0.20	0.13	0.27	0.13
SD	0.07	0.08	0.11	0.07	0.07	0.09	0.07	0.11	0.19	0.09
5th percentile	0.08	0.06	0.05	0.05	0.12	0.01	0.09	0.01	0.01	0.01
95th percentile	4.34	0.26	0.39	0.32	0.38	0.28	0.32	0.32	0.61	0.28
<i>N</i>	16 500	13 900	14 100	2560	7620	11 260	8860	8950	12 600	12 100
NO										
Mean	3.83	2.06	17.46	8.81	13.20	4.80	2.20	1.77	14.45	12.45
Median	3.46	2.44	16.19	7.76	12.43	3.41	2.38	1.91	15.37	11.98
SD	2.16	2.50	7.42	1.88	8.60	3.61	1.22	1.42	10.21	8.99
5th percentile	1.06	0.70	3.49	1.91	1.98	1.23	0.23	0.30	1.44	1.96
95th percentile	7.82	7.94	25.71	7.44	21.33	12.17	3.84	3.97	29.87	26.41
<i>N</i>	82 500	69 500	70 500	12 800	38 100	56 300	44 300	44 750	63 000	60 500
NO₂										
Mean	15.19	11.99	22.95	18.64	21.02	12.17	6.34	7.70	18.87	17.85
Median	13.59	11.44	26.54	22.13	20.23	10.65	6.65	9.11	18.67	16.32
SD	6.10	8.29	13.17	7.89	6.38	7.31	2.77	5.07	10.92	9.87
5th percentile	7.56	7.91	11.45	10.21	6.03	3.65	1.84	1.20	3.86	4.58
95th percentile	26.49	31.90	52.13	35.08	25.97	19.60	3.84	14.75	32.73	31.34
<i>N</i>	82 500	69 500	70 500	12 800	38 100	56 300	44 300	44 750	63 000	60 500
NO_x										
Mean	19.02	16.05	40.41	27.45	34.3	16.97	8.54	9.48	34.74	30.3
Median	17.49	17.91	36.02	26.78	32.40	15.95	9.07	11.27	38.79	28.9
SD	7.96	10.39	19.87	9.67	15.20	8.50	3.94	6.44	20.39	8.66
5th percentile	8.71	9.00	15.53	12.16	9.35	5.20	2.21	1.33	5.77	8.41
95th percentile	33.62	39.36	76.08	42.69	44.54	30.04	13.61	18.57	61.67	45.67
<i>N</i>	82 500	69 500	70 500	12 800	38 100	56 300	44 300	44 750	63 000	60 500

Airborne
determination of the
temporo-spatial
distribution

M. D Shaw et al.

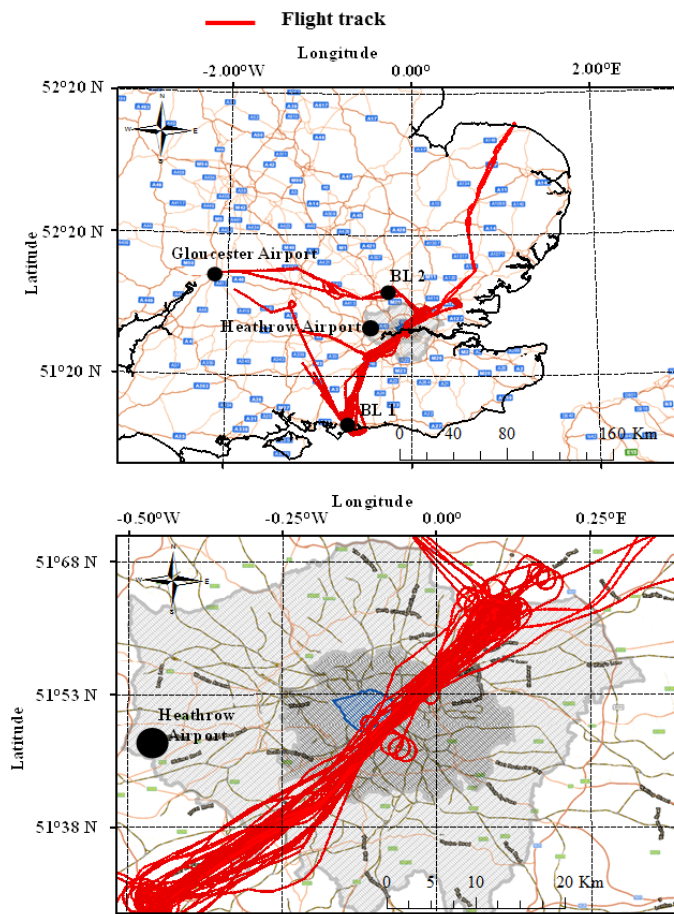


Figure 1. Top: map showing all NERC Dornier-228 flights overlaid on UK transport map. Bottom: total flight legs across Greater London. Grey area; Greater London boundary, black area; inner London boundary, blue area; London CCZ.

Airborne
determination of the
temporo-spatial
distribution

M. D Shaw et al.

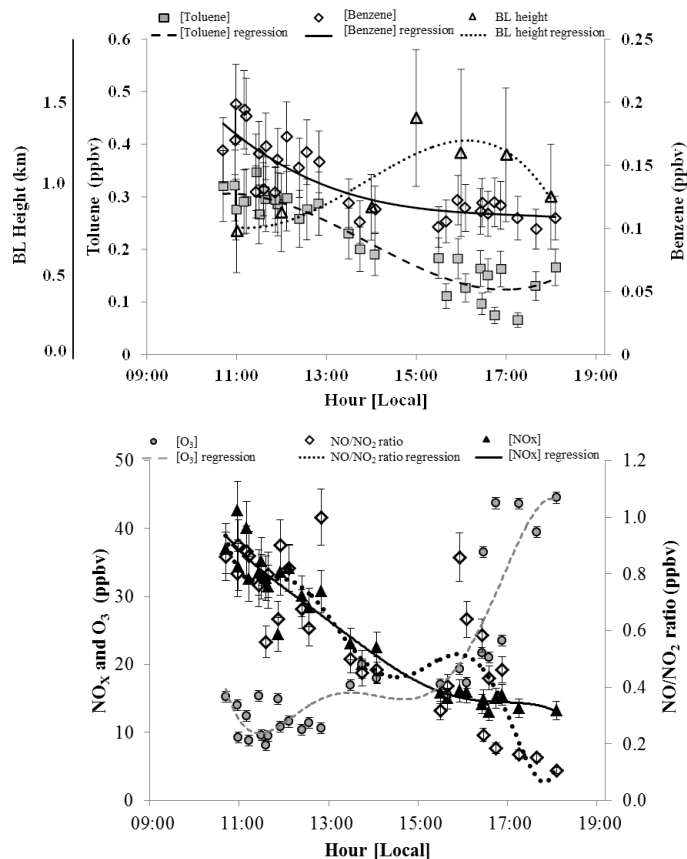


Figure 2. Top: time series of averaged benzene and toluene concentrations observed at 360 ± 10 m a.g.l. during RF 2–6. Bottom: times series of averaged NO/NO₂ ratios and O₃, NO_x concentrations during RF 2–6.

Airborne determination of the temporo-spatial distribution

M. D Shaw et al.

Title Page

Abstract

Introduction

Conclusions

References

Tables

Figures



Back

Close

Full Screen / Esc

Printer-friendly Version

Interactive Discussion

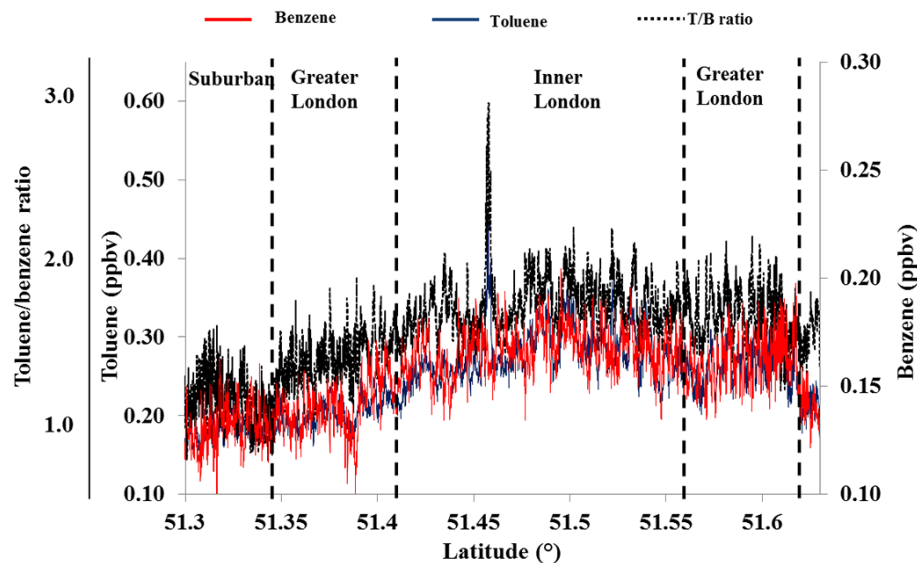


Figure 3. City cross section of 1 km averaged benzene, toluene mixing ratios and T/B instantaneous ratios (ppbv ppbv⁻¹) at 360 ± 10 m a.g.l. across Greater London during RF 5.

Airborne
determination of the
temporo-spatial
distribution

M. D Shaw et al.

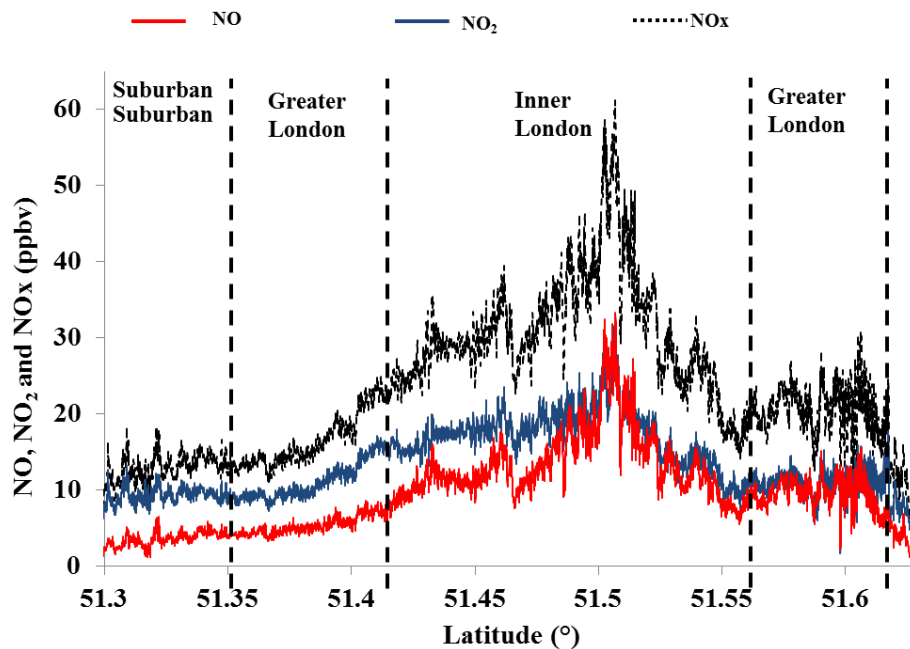


Figure 4. City cross section of 1 km averaged NO, NO₂ and NO_x mixing ratios across Greater London at 360 ± 10 m a.g.l. during RF 5.

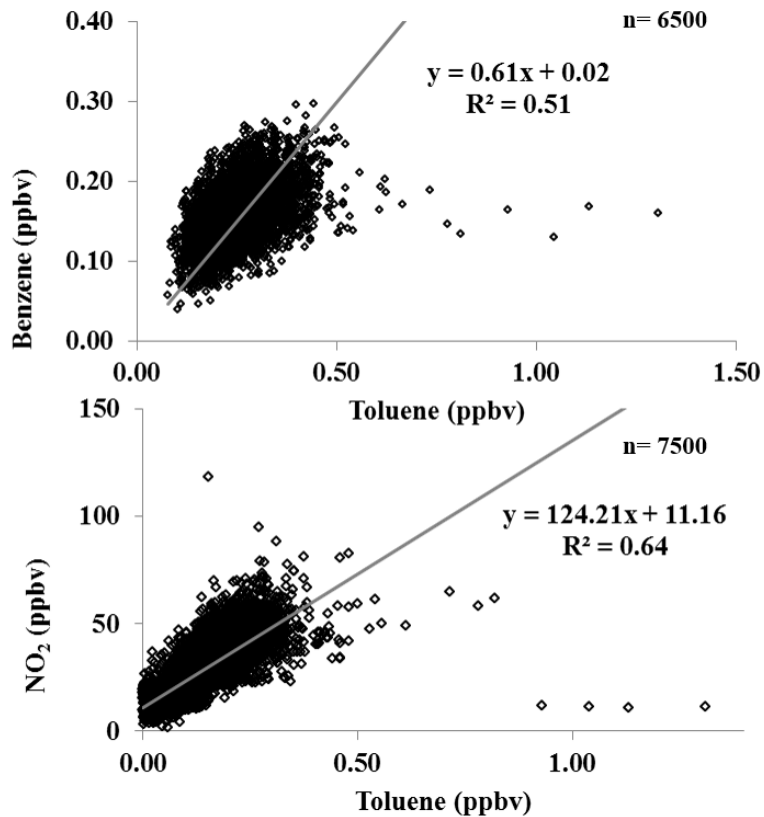


Figure 5. Top: linear regression analysis of benzene against toluene mixing ratios at 360 ± 10 m a.g.l. during RF 5. Bottom: linear regression analysis of NO_2 against toluene mixing ratios at 360 ± 10 m a.g.l. during RF 5.

Airborne
determination of the
temporo-spatial
distribution

M. D Shaw et al.

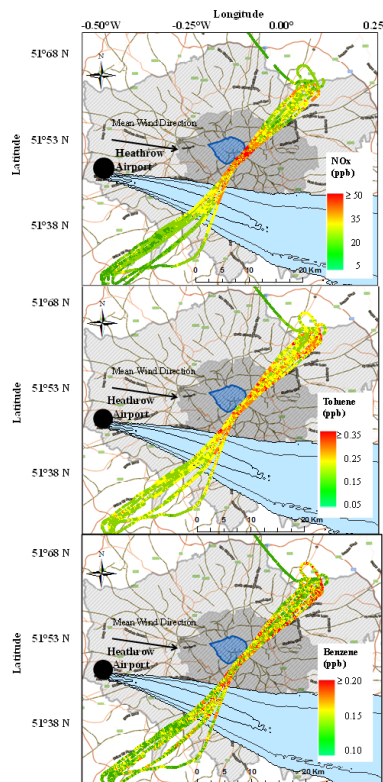


Figure 6. Top: NO_x concentration data (7 m resolved at 360 ± 10 m a.g.l.) during RF5 overlaid on UK transport map. Middle: Benzene concentration data (35 m resolved at 360 ± 10 m a.g.l.) during RF5 overlaid on UK transport map. Bottom: Toluene concentration data (35 m resolved at 360 ± 10 m a.g.l.) during RF5 overlaid on UK transport map. Grey area; Greater London boundary, black area; inner London boundary, dark blue area; London CCZ, light blue area; 3 h averaged HYSPLIT dispersion trajectory.

Title Page

Abstract

Introduction

Conclusions

References

Tables

Figures



Back

Close

Full Screen / Esc

Printer-friendly Version

Interactive Discussion



**Airborne
determination of the
temporo-spatial
distribution**

M. D Shaw et al.

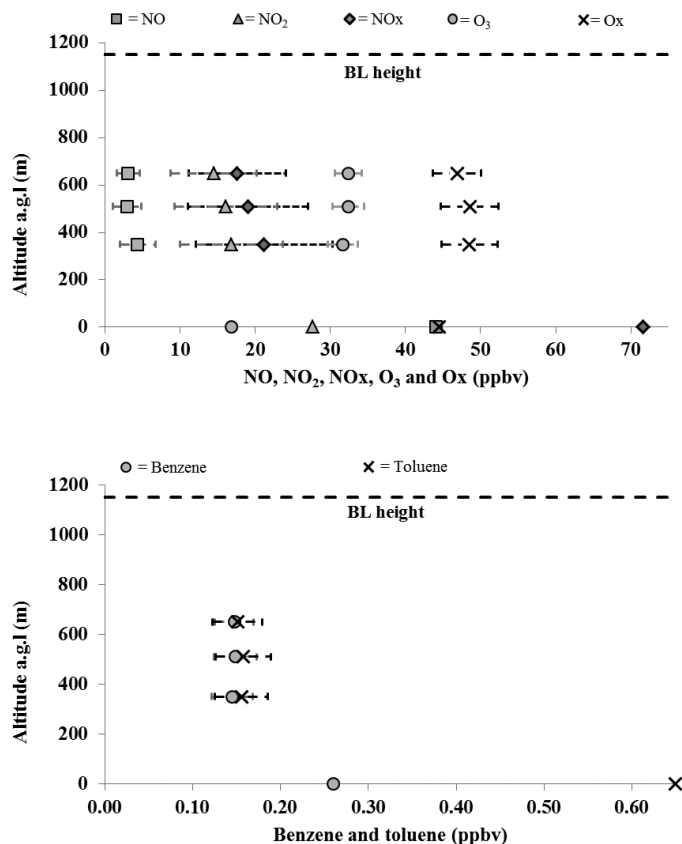


Figure 7. Average vertical profiles of O_3 , NO , NO_2 , O_x , benzene and toluene across London during RF1, 17:00–18:00LT on the 24 June 2013. X error bars represent standard deviation (1σ) of mixing ratios observed during each flight leg. Mixing ratio at ground level is hourly average from the LAQN Marylebone road air quality monitoring station.

Title Page

Abstract

Introduction

Conclusions

References

Tables

Figures

◀

▶

◀

▶

Back

Close

Full Screen / Esc

Printer-friendly Version

Interactive Discussion



Airborne determination of the temporo-spatial distribution

M. D Shaw et al.

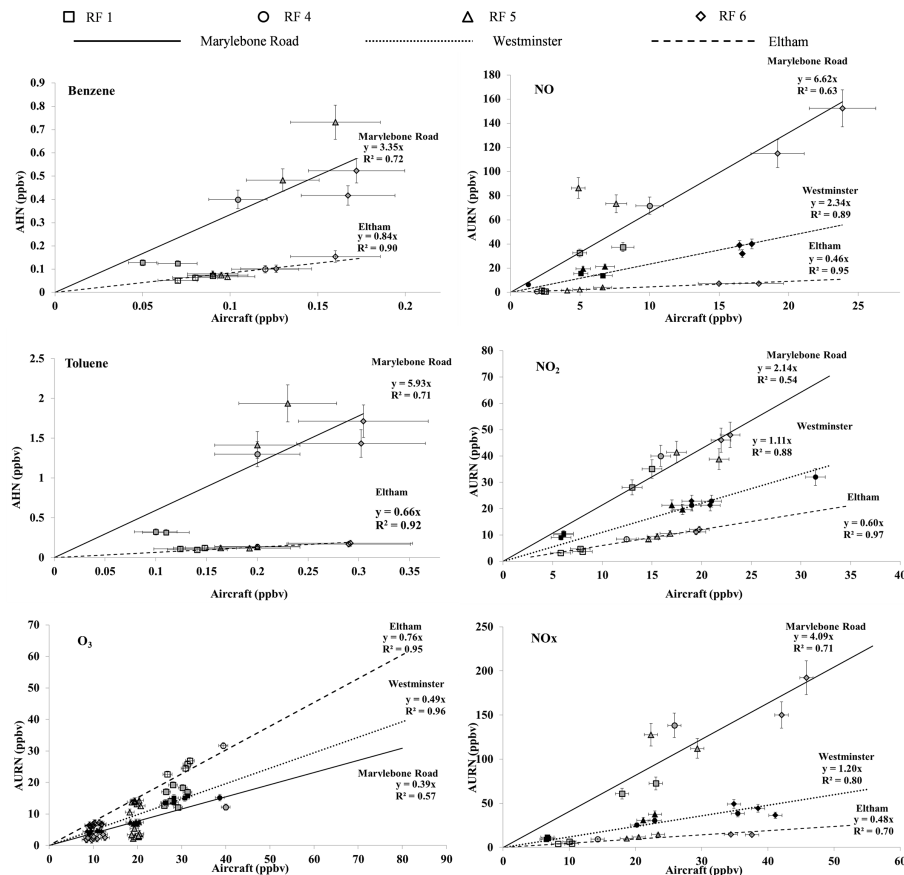


Figure 8. Linear regression analysis between airborne (at 360 ± 10 m a.g.l.) and hourly ground measurements at Greenwich–Eltham, Westminster–Horseferry road and Marylebone Road from the LAQN monitoring network during RF1, 4, 5 and 6.



Title Page

Abstract

Introduction

Conclusions

References

Tables

Figures

◀

▶

◀

▶

Back

Close

Full Screen / Esc

Printer-friendly Version

Interactive Discussion